Available online at www.sciencedirect.com
SCIENCE DIRECT®
Journal of Organometallic Chemistry 690 (2005) 4745–4754
Journal of Organometallic Chemistry
www.elsevier.com/locate/jorganchem

(Tetramethylcyclobutadiene)cobalt complexes with monoanionic carborane ligands [9-L-7,8-$C_2B_9H_{10}$]$^-$ (L = SMe_2, NMe_3 and py) ☆

Vladimir I. Meshcheryakov [a], Peter S. Kitaev [a], Konstantin A. Lyssenko [a], Zoya A. Starikova [a], Pavel V. Petrovskii [a], Zbyněk Janoušek [b], Maddalena Corsini [c], Franco Laschi [c], Piero Zanello [c], Alexander R. Kudinov [a,*]

[a] *Laboratory of Transition Metal π-Complexes, A. N. Nesmeyanov Institute of Organoelement Compounds, Russian Academy of Sciences, ul Vavilova 28, 119991 Moscow, Russian Federation*
[b] *Institute of Inorganic Chemistry, Academy of Sciences of the Czech Republic, 25068 Řež, Czech Republic*
[c] *Dipartimento di Chimica dell'Università di Siena, Via Aldo Moro, 53100 Siena, Italy*

Received 27 February 2005; received in revised form 19 July 2005; accepted 20 July 2005
Available online 22 September 2005

Abstract

nido-Carborane 9-NMe_3-7,8-$C_2B_9H_{11}$ (**2c**) was synthesized by $CuSO_4$ oxidation of anion [7,8-$C_2B_9H_{12}$]$^-$ in the presence of [Me_3NH]$^+$ in aqueous ammonia. Improved procedures for the preparation of *nido*-carboranes 9-SMe_2-7,8-R_2-7,8-$C_2B_9H_9$ (**2a**: R = H; **2b**: R = Me) and 9-py-7,8-$C_2B_9H_{11}$ (**2d**) were developed. *nido*-Carborane monoanions [9-L-7,8-R_2-7,8-$C_2B_9H_8$]$^-$ (**1a**–**1d**), generated by deprotonation of **2a**–**2d** by NaH, react with Cb*Co(CO)$_2$I or [Cb*Co(MeCN)$_3$]$^+$ (Cb* = C_4Me_4) to give complexes Cb*Co(η-9-L-7,8-R_2-7,8-$C_2B_9H_8$) (**3a**–**3d**). The structures of carborane **2d** and complexes **3a** and **3d** were determined by X-ray diffraction. Electrochemistry of the cobalt complexes was studied.

Keywords: Carboranes; Cobalt; Cyclobutadiene complexes; Electrochemistry; Metallacarboranes; Sandwich compounds

1. Introduction

Cobaltacarboranes are the most studies of metallacarboranes [2]. Overwhelming majority of cobaltacarboranes described are derivatives of carborane dianions and, in particular, of the dicarbollide [7,8-$C_2B_9H_{11}$]$^{2-}$ [3]. The latter is isolobal [4] with the Cp^- anion but has a different charge, resulting in significant difference in the properties of dicarbollyl and cyclopentadienyl derivatives. In order to obtain closer metallacarborane analogues of cyclopentadienyl complexes, we used charge-compensated dicarbollide monoanions [9-L-7,8-R_2-7,8-$C_2B_9H_8$]$^-$ (**1a**–**1d**); **a**: L = SMe_2, R = H [5]; **b**: L = SMe_2, R = Me; **c**: L = NMe_3, R = H; **d**: L = py, R = H [6]), which are not only isolobal with Cp^- but also have the same charge.

Many transition metal derivatives of charge-compensated dicarbollide monoanions, mainly of **1a** [7], have been prepared earlier. However, only a few examples of cobalt complexes with such ligands were described. For instance, Plešek et al. [5a] have synthesized compound (η-7,8-$C_2B_9H_{11}$)Co(η-9-SMe_2-7,8-$C_2B_9H_{10}$) containing both carborane mono- and dianions. Hawthorne et al. [8] have prepared the bis(dicarbollyl) complex [Co{η-9-(4-CO_2Me-C_5H_4N)-7,8-$C_2B_9H_{10}$}$_2$]$^+$ with methylnicotinate as a substituent.

Herein, we describe simple procedures for the preparation of the starting charge-compensated carboranes

☆ (Tetramethylcyclobutadiene)cobalt Complexes, 3. Part 2: Ref. [1].

* Corresponding author. Tel.: +7 095 135 9367; fax: +7 095 135 5085.
E-mail addresses: zanello@unisi.it (P. Zanello), arkudinov@ineos.ac.ru (A.R. Kudinov).

0022-328X/$ - see front matter © 2005 Elsevier B.V. All rights reserved.
doi:10.1016/j.jorganchem.2005.07.067

9-L-7,8-R_2-7,8-$C_2B_9H_9$ (**2a**–**2d**) including two new derivatives **2b** and **2c**. Synthesis and electrochemical behaviour of the (tetramethylcyclobutadiene)cobalt complexes Cb*Co(η-9-L-7,8-R_2-7,8-$C_2B_9H_8$) (**3a**–**3d**); Cb* = C_4Me_4) as well as the structures of **2d**, **3a** and **3d** are also reported.

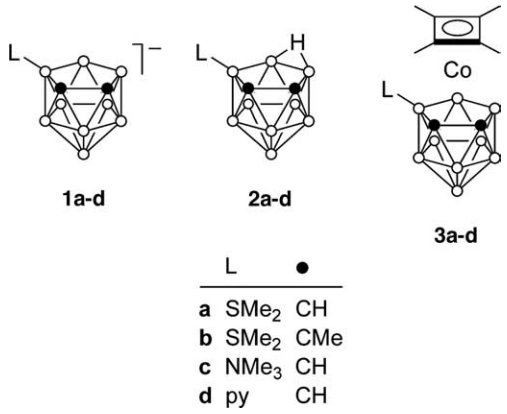

2. Results and discussion

2.1. Synthesis of charge-compensated carboranes *2a–2d* and anionic ligands *1a–1d*

For the preparation of the Me_2S-substituted carborane **2a** [9], Plešek et al. [5a] have developed a simple method based on the reaction of the potassium salt of anion [7,8-$C_2B_9H_{12}$]$^-$ with DMSO in aqueous H_2SO_4 at room temperature. However, sometimes this procedure is not reproduced. This trouble can be avoided by carrying out the reaction at elevated temperature (80 °C) as it was proposed by Mingos et al. [5b]. Based on this improvement, we prepared **2a** in one-pot starting from *ortho*-carborane. The potassium salt K[7,8-$C_2B_9H_{12}$], formed by decapitation of 1,2-$C_2B_{10}H_{12}$ by KOH in MeOH, was not isolated in pure form but used as a mixture with an excess of KOH (after evaporation of MeOH) for further reaction with DMSO/H_2SO_4. The dimethylated analogue **2b** was prepared similarly from 1,2-Me_2-1,2-$C_2B_{10}H_{10}$.

The 9-NMe_3-substituted carborane (**2c**) was earlier unknown. The 10-NEt_3-analogue 10-NEt_3-7,8-$C_2B_9H_{11}$ has been prepared by Hawthorne et al. [8] in a very low yield (4%) by oxidation of anion [7,8-$C_2B_9H_{12}$]$^-$ with $FeCl_3$ in the presence of NEt_3; the major product was the ferracarborane [Fe(η-7,8-$C_2B_9H_{11}$)$_2$]$^{2-}$ formed as a result of deprotonation of [7,8-$C_2B_9H_{12}$]$^-$ by NEt_3 and subsequent coordination with the Fe^{2+} cation. In order to avoid the formation of a metallacarborane, we used $CuSO_4$ as an oxidant in the reaction of [7,8-$C_2B_9H_{12}$]$^-$ with NMe_3 (generated from [Me_3NH]$^+$) in aqueous ammonia (Scheme 1). Much lower π-coordinating ability of the Cu^{2+} cation compared with Fe^{2+} allowed to prepare carborane **2c** in a high yield (85–90%).

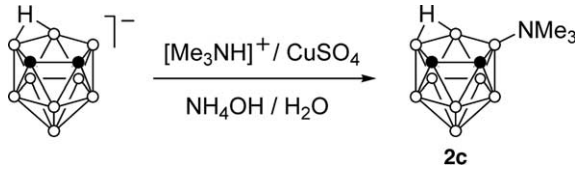

Scheme 1.

Using the reaction of [7,8-$C_2B_9H_{12}$]$^-$ with $FeCl_3$ in the presence of pyridine in refluxing benzene, Hawthorne et al. [6] have isolated (after recrystallization) the pyridine-substituted carborane **2d** as a bright yellow solid. Carrying out this reaction in net pyridine with the use of $FeCl_3 \cdot 6H_2O$ instead of anhydrous $FeCl_3$ (Scheme 2), we noticed that the yellow colour of the product is caused by an admixture of a minor product which can be removed by column chromatography on silica gel. Pure carborane **2d** proved to be colourless in the solid state and very pale yellow in solution. Based on the ^1H and ^{11}B NMR data, the yellow minor product was supposed to be the bis(pyridine)-substituted carborane 9,11-py_2-*nido*-7,8-$C_2B_9H_9$.

For further synthesis of cobaltacarboranes **3a**–**3d**, we used sodium derivatives of anions **1a**–**1d**. Compounds Na[**1a**] [5a] and Na[**1d**] [6] have been prepared earlier by deprotonation of **2a** and **2d** with NaH in THF. We used analogous reactions of **2b**, **2c** for the preparation of Na[**1b**,**c**]. The NMe_3-derivative **2c** proved to be less reactive than the other carboranes, apparently owing to its lower acidity as a consequence of greater steric effect and donor ability of the NMe_3 substituent compared with SMe_2 and py. Based on a single crystal X-ray diffraction study, we have established that the sodium derivatives of anions **1a**, **1c** and **1d** have a dimeric structure in the solid state [10].

2.2. Synthesis of complexes *3a–3d*

Cobaltacarboranes having the cyclobutadiene ring at the metal atom were previously unknown. We prepared the first examples of such compounds, complexes **3a**–**3d**, using reactions of anions **1a**–**1d** with Cb*Co(CO)$_2$I or [Cb*Co(MeCN)$_3$]$^+$ (Scheme 3) [11]. The reaction of sodium derivatives of anions **1a**, **1c**, **1d** with the (carbonyl)iodide complex Cb*Co(CO)$_2$I affords

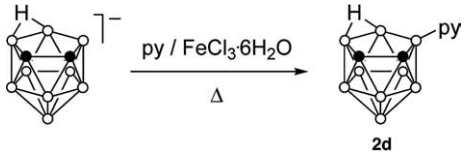

Scheme 2.

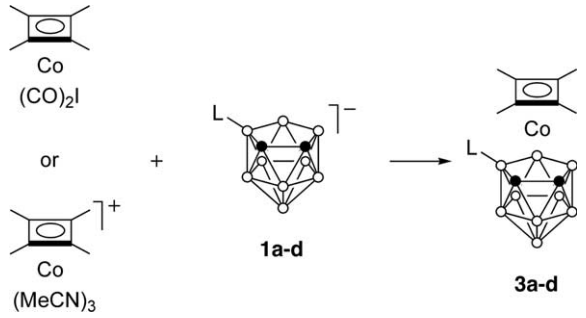

Scheme 3.

cobaltacarboranes **3a**, **3c**, **3d** in moderate yields after refluxing for several hours in THF; the yields of **3a**, **3d** were increased using thallium derivatives Tl[**1a**,**d**] [12] due to the abstraction of the iodide anion by Tl^+. The reaction of Na[**1a**–**d**] with the more electrophilic acetonitrile complex $[Cb^*Co(MeCN)_3]^+$ (generated by heating or visible light irradiation of the arene complex $[Cb^*Co(C_6H_6)]^+$ or $[Cb^*Co(C_6H_5Me)]^+$ in MeCN [1,13]) readily proceeds at room temperature and gives **3a**–**3d** in high yields.

Complexes **3a**–**3d** are air-stable yellow-orange solids. They can be considered as metallacarborane analogues of cyclopentadienyl complexes $Cb^*Co(C_5R_5)$ [1,14]. In accordance with this analogy, complexes of both types are formed in identical conditions and exhibit very similar electrochemical behaviour (vide infra).

The ^1H NMR spectra of **3a**–**3d** contain singlets of the Cb* methyl groups, two broad singlets of cage CH or CMe protons and signals of charge-compensating substituent L. In the ^{11}B NMR spectra, there are eight or nine signals; only one of them, assigned to the boron atom bonded with substituent L, is not coupled with ^1H.

2.3. Structures of nido-carborane *2d* and complexes *3a* and *3d*

The structures of *nido*-carborane **2d** and complexes **3a** and **3d** determined by X-ray diffraction are shown in Figs. 1 and 2. Selected bond lengths and angles are given in Table 1; the table also quotes data for *nido*-carborane **2a** [15]. Like in the works of Stone and Jelliss [16], the atom numbering in the cobalt complexes and the starting carboranes is similar, facilitating comparison of their structures.

Comparison of bond lengths for **2a** and **2d** revealed that although they are close, there are some distinct differences in bond lengths in the open face. The μ_2-hydrogen atom is located above the B(10)–B(11) bond in an asymmetrical manner. This bond is considerably longer than the other B–B bonds owing to its loosening caused by bonding of the B(10) and B(11) atoms with proton. The C_2B_3-pentagonal edge is characterized by flattened envelope conformation with the deviation of the C(7) atom by 0.08 Å both in **2a** and **2d**.

The character and magnitude of the bond elongation/shortening in the C_2B_3 face of the cobalt complexes **3a** and **3d** in comparison with the *nido*-carboranes are similar in both cases. The C_2B_3 edge becomes almost planar in the complexes with maximum deviation of the B(10) (**3a**) and B(11) (**3d**) atoms by 0.04 Å. The bonds B(9)–N(1)/S(1) are practically the same in **2a**, **2d** and **3a**, **3d**. The C(7)–C(8) bond in the pyridine derivatives **2d** and

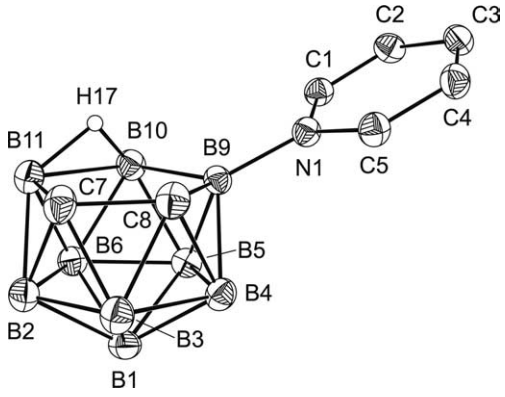

Fig. 1. Structure of carborane **2d**. Atoms are represented by 50% thermal ellipsoids.

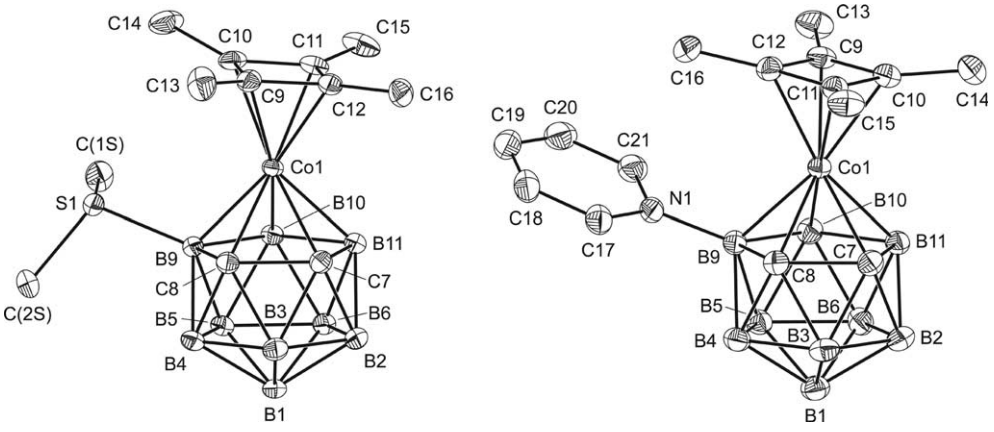

Fig. 2. Structures of complexes **3a** (left) and **3d** (right). Atoms are represented by 50% thermal ellipsoids.

Table 1
Selected bond lengths (Å) for **2a**,[a] **2d**, **3a** and **3d**

	2a	2d	3a	3d
Co(1)–C(7)			2.0274(8)	2.002(2)
Co(1)–C(8)			2.0312(7)	2.008(2)
Co(1)–B(9)			2.0635(8)	2.064(2)
Co(1)–B(10)			2.1178(8)	2.123(2)
Co(1)–B(11)			2.0747(8)	2.080(2)
Co(1)–C(9)			2.0027(7)	1.982(2)
Co(1)–C(10)			2.0057(8)	1.996(2)
Co(1)–C(11)			1.9824(8)	1.999(2)
Co(1)–C(12)			2.0017(7)	2.003(2)
C(7)–C(8)	1.528(4)	1.551(3)	1.628(1)	1.642(3)
C(7)–B(11)	1.618(5)	1.631(3)	1.704(1)	1.698(3)
C(8)–B(9)	1.576(4)	1.597(3)	1.692(1)	1.702(3)
B(9)–B(10)	1.774(4)	1.788(3)	1.773(1)	1.762(3)
B(10)–B(11)	1.847(5)	1.859(3)	1.793(1)	1.784(3)
B(9)–N(S)(1)	1.884(3)	1.546(2)	1.9017(8)	1.548(3)
B(10)–H(17)	1.17(3)	1.20(3)		
B(11)–H(17)	1.35(3)	1.29(3)		

[a] Ref. [15].

3d is considerably longer (by 0.024(3) and 0.014(3) Å, respectively) than that in the SMe_2-substituted analogues **2a** and **3a**, thus indicating that the exchange of pyridine for SMe_2 group leads to some redistribution of charge in the C_2B_3 open face.

The dihedral angle between the C_4 and C_2B_3 planes for **3a** (6.8°) is greater than that for **3d** (4.7°), apparently owing to greater steric overcrowding caused by the SMe_2 substituent in comparison with pyridine. The mutual disposition of the Cb* and C_2B_3 rings in **3a** and **3d** is slightly different. In **3a**, one of the cyclobutadiene carbon atoms is located above the C(8) atom, whereas in **3d** it is located above B(10).

Although the Co–B distances in **3a** and **3d** are practically the same, the Co(1)–C(7) and Co(1)–C(8) bonds in **3a** are systematically longer than in **3d**, resulting in elongation of the Co···C_2B_3 distance in **3a** (1.457 Å) compared to **3d** (1.445 Å). It suggests the stronger bonding of the Co atom with the pyridine-substituted carborane ligand **1a**. Interestingly, the Co···C_2B_3 distance in **3a** is slightly shorter than the corresponding values for the bis(carboranyl) complexes DD/LL-[Co(η-9-SMe_2-7,8-$C_2B_9H_{10})_2]^+$ (1.482–1.492 Å; av. 1.487 Å) and *meso*-[Co(η-9-SMe_2-7,8-$C_2B_9H_{10})_2]^+$ (1.485–1.494; 1.489 Å) [17], which is apparently connected with greater back-donation in the case of **3a** due to donor effect of the Cb* ligand.

The cyclobutadiene fragment is nearly square planar with the sides ca. 1.456 (**3a**) and 1.452 (**3d**) Å, very close to the value 1.453 Å observed for the acetylcyclopentadienyl complex Cb*Co(η-C_5H_4COMe) (**4**). The carbon atoms of the Cb* methyl groups in **3a** and **3d** are somewhat deviated from the ring planes in direction from the cobalt atom; the deviations amount to 0.13–0.39 and 0.11–0.27 Å, respectively. These deviations are slightly greater than those for **4** (0.08–0.17 Å). The cobalt atoms are located over the centers of the Cb* rings; the Co···Cb* distances in **3a** (1.712 Å) and **3d** (1.711 Å) are considerably longer than the corresponding distance in **4** (1.683 Å). Probably, it is connected with lower back-donation due to the greater acceptor properties of carborane ligands compared with cyclopentadienyl.

2.4. Electrochemistry and spectroelectrochemistry

In CH_2Cl_2 solution, complexes **3a**–**3d** undergo an oxidation process showing features of chemical reversibility in the cyclic voltammetric time scale. In all cases, controlled potential coulometry consumed one electron *per* molecule and cyclic voltammetric tests on the resulting solutions afforded voltammetric profiles quite complementary to the original ones, thus testifying for the complete stability of all the corresponding monocations. Analysis of the cyclic voltammetric responses with scan rate varying from 0.02 to 2.00 V s^{-1} pointed out the occurrence of a diffusion-controlled electron removal (the current function $i_{pa}v^{-1/2}$ maintains substantially constant with scan rate) possessing features of chemical reversibility (as a matter of fact, in agreement with macroelectrolysis tests, the current ratio i_{pc}/i_{pa} is constantly equal to 1) and electrochemical quasireversibility (ΔE_p significantly departs from the theoretical value of 59 mV even at the lowest scan rates) [18]. The potential values of such an anodic process, which is preliminarily assigned as the Co(I)/Co(II) redox change, are compiled in Table 2. A further, irreversible, multielectron oxidation is present at notably higher potential values (from +1.6 to +1.7 V, depending upon the different species), which probably couples the Co(II)/Co(III) passage to ligand-centered electron transfers. It is noteworthy that the presence or the absence of the electron-donating methyl substituents on the 7,8-carbon atoms does not affect the Co(I)/Co(II) oxidation (**3a** vs. **3b**), whereas the 9-boron substituents exert their inductive effects. Interestingly, the first oxidation processes for **3a**–**3d** proceed at the potentials very close to that of Cb*CoCp (+0.51 V) [1], suggesting the similarity of donor–acceptor properties of ligands **1a**–**1d** and Cp^-.

The typical optical absorption accompanying the progressive Co(I)/Co(II) oxidation is illustrated in Fig. 3, which shows the spectroelectrochemical picture

Table 2
Formal electrode potentials (V, vs. SCE) and peak-to-peak separations (mV) for the chemically reversible oxidation exhibited by complexes under study in CH_2Cl_2 solution

Complex	$E^{o\prime}_{(0/+)}$	ΔE_p[a]
3a	+0.57	80
3b	+0.57	75
3c	+0.50	78
3d	+0.54	91

[a] Measured at 0.05 V s^{-1}.

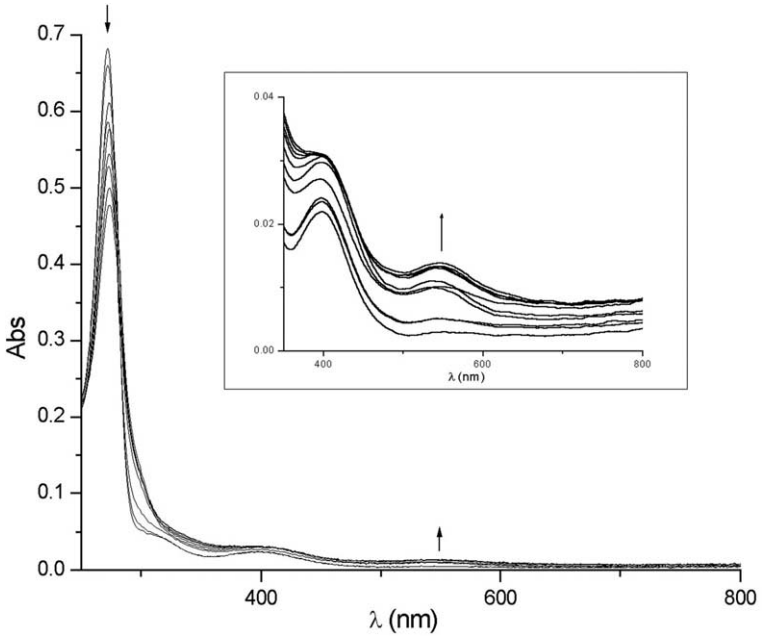

Fig. 3. Spectral changes recorded at room temperature in an OTTLE cell upon progressive one-electron oxidation of complex **3c** (1.4×10^{-3} mol dm^{-3}). CH_2Cl_2 solution containing $[NBu_4]PF_6$ (0.2 mol dm^{-3}). Working potential, $E_w = +0.5$ V, vs. Ag-pseudoreference electrode.

obtained for complex **3c** in an OTTLE (optically transparent thin-layer electrode) cell. As seen, the progressive decrease of the band at 400 nm upon oxidation is accompanied by the appearance of a new band at 535 nm, which is assigned to a d–d transition. The data pertinent to all the complexes are summarized in Table 3, together with the colour changes recorded upon exhaustive oxidation.

Fig. 4 shows the X-band EPR spectrum of the monocation $[\mathbf{3d}]^+$ in a frozen CH_2Cl_2 solution. The spectral analysis is suitably performed assuming that the Co(II) metal ion lies in the low spin $S = 1/2$ electronic state. Under the assumption of an anisotropic electron spin Hamiltonian, the lineshape appears resolved in widely separated pseudo-axial absorptions. In fact, the high-field spectral region exhibits two closely overlapped g_i signals, g_m and g_h [19], the pseudo-axial g_i parameters of which testify for the important metallic character of the paramagnetic absorption ($g_l \gg g_m \geqslant g_h \neq g_{electron} = 2.0023$). On the other hand, the broad linewidth in the g_l low-field region is due to either the noticeable magnetic coupling of the $S = 1/2$ unpaired

Table 3
Colour changes and quantitative spectrophotometric data accompanying the exhaustive one-electron oxidation of complexes **3a**–**3d** in CH_2Cl_2 solution

Complex	Colour	λ_{max}	Complex	Colour	λ_{max}
3a	Yellow	390	$[\mathbf{3a}]^+$	Orange	530
3b	Yellow	390	$[\mathbf{3b}]^+$	Red	540
3c	Yellow	400	$[\mathbf{3c}]^+$	Red	535
3d	Yellow-orange	380	$[\mathbf{3d}]^+$	Pink	540

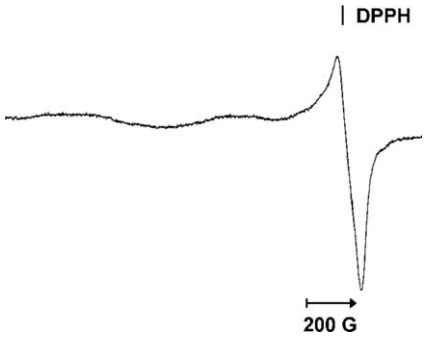

Fig. 4. First derivative, X-band EPR spectrum of the electrogenerated monocation $[\mathbf{3d}]^+$ in CH_2Cl_2 solution. $T = 105$ K.

electron with the metal nucleus or the concomitant strong Co(II) spin orbit contribution to the actual paramagnetic features ($\lambda_{Co} < 0$). Accordingly, the relevant anisotropic Co hyperfine splittings (hpf) are not resolved [$I(^{59}Co) = 7/2$, natural abundance = 100%] and an upper limit for such strong magnetic interaction is of the order $\Delta H_l = 320(8)$ G $\leqslant 7a_l$(Co).

These features well account for a SOMO, which is mainly constituted by the $3d^7$ Co(II) orbitals. Because of the anisotropic ΔH_i overlapping of the underlying absorptions, there is no evidence for superhyperfine (shpf) interactions of the unpaired electron with the magnetically active ^{1}H, ^{10}B and ^{11}B nuclei of the axial ligands ($\Delta H_i \geqslant a_i$).

Rising the temperature at the glassy-fluid transition ($T = 278$ K), the anisotropic spectrum collapses in an isotropic signal ($g_{iso} = 2.296(8)$), which maintains the metallic character. At higher temperature ($T = 300$ K)

Table 4
X-band EPR parameters of the monocations under study in CH_2Cl_2 solution. $T = 100$ K

Complex	g_l	g_m	g_h	$\delta g_{l/h}$	$<g>$	a_l	a_m	a_h	$\langle a \rangle$
$[\mathbf{3a}]^+$		1.999	1.955				⩽95/7	⩽95/7	
$[\mathbf{3b}]^+$	2.967	2.002	1.961	1.006	2.310	⩽270/7	⩽140/7	⩽140/7	⩽137/7
$[\mathbf{3c}]^+$	3.031	1.979	1.922	1.109	2.311	⩽320/7	⩽100/7	⩽100/7	⩽140/3
$[\mathbf{3d}]^+$	2.990	1.996	1.960	1.030	2.315	⩽320/7	⩽95/7	⩽95/7	⩽138/7

Accuracy of $g_i = \pm 0.008$. Accuracy of $a_i = \pm 8$ G.
$\langle g \rangle = (g_l + g_m + g_h)/3$; $\langle a \rangle = (a_h + a_m + a_h)/3$; $a_i(\mathrm{Co}) \leqslant \Delta H_i/7$ in Gauss.

the spectrum drops out, indicating that the active fastening of the $S = 1/2$ electron spin relaxation rates enhances the effective linebroadening effect. The lack of Co(II) hpf resolution in fluid solution is not surprising in view of the large Co(II) spin–orbit coupling constant (<0) and the expected structural anisotropies (being the coordinating framework basically unsymmetrical even in fast motion conditions), which fasten the relevant electron spin relaxation rates [19,20]. Accordingly, no resolution of the magnetically active ^1H, ^{13}C, ^{10}B, ^{11}B ligand nuclei is detectable, so that the upper limit for such interactions can be evaluated as: $a_{iso}(^1H, ^{13}C, ^{10}B, ^{11}B) \leqslant \Delta H_{iso} = 170(8)/7$ G.

The most significant EPR features are summarized in Table 4, together with those of the other monocations. The good accordance between the $\langle g \rangle$ and g_{iso} parameters indicates that the monocation $[\mathbf{3d}]^+$ basically maintains the coordination geometry under different experimental conditions. In confirmation, rapidly refreezing the fluid solution restores the original pseudoaxial anisotropic spectrum.

Analysis of the magnetic parameters suggests that the SOMOs of all the monocations are essentially 3d centered. It is also evident that the steric encumbrance of the substituents present in the carborane ligand strongly affects the magnetic features, as supported by the anisotropic g_i and $\delta g_{l/h}$ parameters [19,20]. In particular, $[\mathbf{3c}]^+$ exhibits the highest g_l and $\delta g_{l/h}$ values, thus reflecting the presence of the most significant structural distortions. Such a finding is further confirmed by the lack of the relevant fluid solution isotropic features. This last aspect also holds for $[\mathbf{3a}]^+$ and $[\mathbf{3b}]^+$.

3. Conclusion

(Cyclobutadiene)cobaltacarboranes **3a**–**3d** were prepared by reactions of complexes $Cb^*Co(CO)_2I$ and $[Cb^*Co(MeCN)_3]^+$ with the corresponding anions, illustrating usefulness of this approach in metallacarborane chemistry. Proximity of oxidation potentials of complexes **3a**–**3d** and Cb*CoCp suggests very similar donor–acceptor ability of anions **1a**–**1d** and Cp^-.

4. Experimental

4.1. General

All reactions were carried out under argon. The isolation of products was conducted in air unless otherwise stated. The starting materials $Cb^*Co(CO)_2I$, $[Cb^*Co(C_6H_6)]PF_6$ and $[Cb^*Co(C_6H_5Me)]PF_6$ were prepared as described in the literature [1]. The ^1H and ^{11}B NMR spectra (δ in ppm, J in Hz) were recorded with a Bruker AMX 400 spectrometer operating at 400.13 and 128.38 MHz, respectively.

Materials and apparatus for electrochemistry and joint EPR spectroscopy have been described elsewhere [21]. Unless otherwise specified, potential values are referred to the saturated calomel electrode (SCE). Under the present experimental conditions, the one-electron oxidation of ferrocene occurs at $E^{\circ\prime} = +0.39$ V. The UV–Vis spectroelectrochemical measurements were carried out using a Perkin–Elmer Lambda 900 UV–Vis spectrophotometer and an OTTLE cell [22] equipped with a Pt-minigrid working electrode (32 wires/cm), Pt minigrid auxiliary electrode, Ag wire pseudoreference and CaF_2 windows. The electrode potential was controlled during electrolysis by an Amel potentiostat 2059 equipped with an Amel function generator 568. Nitrogen-saturated solutions of the compounds under study were used with $[NBu_4]PF_6$ (0.2 mol dm^{-3}) as a supporting electrolyte. Working potential has been kept fixed at the peak potential of the process under study and the spectra have been stepwise collected after each 2 min electrolysis.

4.2. Synthesis of 9-SMe_2-7,8-$C_2B_9H_{11}$ (**2a**)

Under stirring and cooling by cold water, *o*-carborane (14.4 g, 0.10 mmol) was slowly added to a solution of KOH (15 g, 0.27 mmol) in 100–150 ml of MeOH placed in a 0.5 L flask. Vigorous reaction takes place spontaneously. The reaction mixture was stirred at room temperature until hydrogen evolution was over and was then refluxed for 4 h. The most of MeOH was removed by distillation at atmospheric pressure, water (150–170 ml) was added and the rest of the MeOH

was removed by evaporation in vacuum to give an aqueous alkaline solution of $K[C_2B_9H_{12}]$. DMSO (25 ml) was added followed by dropwise addition of conc. H_2SO_4 (160 ml). The reaction mixture was heated at 80 °C for 1 h leading to the formation of the white oily layer, which solidifies after cooling to room temperature. The product was separated, washed subsequently with water, diluted Na_2CO_3 solution and water, and recrystallized from hot MeOH. After standing overnight at 0 °C, the crystalline product was filtered off, washed with a small amount of Et_2O and dried in vacuum. Yield 13.5 g (70%). M.p. 147–148 °C. ^{1}H NMR (acetone-d_6): $\delta = 2.86$ (s, 3H, SMe_2), 2.79 (br s, 1H, cage CH), 2.73 (s, 3H, SMe_2), 2.15 (br s, 1H, cage CH), −3.27 (v br s, 1H, μ-H). ^{11}B NMR (acetone-d_6): $\delta = -3.53$ (d, 142, 1B), −5.34 (s, $BSMe_2$, 1B), −11.79 (d, 155, 1B), −15.92 (d, 193, 1B), −17.64 (d, 182, 1B), −22.54 (d, 153, 1B), −25.71 (d, 144, 1B), −29.35 (d, 133, 1B), −36.15 (d, 146, 1B).

4.3. Synthesis of 9-SMe_2-7,8-Me_2-7,8-$C_2B_9H_9$ (**2b**)

Compound **2b** was prepared starting from 1,2-Me_2-1,2-$C_2B_{10}H_{10}$ similar to the previous procedure but using ethanol instead of methanol. The crude product was recrystallized from hot hexane. Yield 64%. ^{1}H NMR ($CDCl_3$): $\delta = 2.74$ (s, 3H, SMe_2), 2.57 (s, 3H, SMe_2), 1.57 (s, 3H, cage CMe), 1.50 (s, 3H, cage CMe), −3.15 (v br s, 1H, μ-H). ^{11}B NMR ($CDCl_3$): $\delta = -5.96$ (s, 1B, $BSMe_2$), −6.70 (d, 154, 1B), −7.87 (d, 155, 1B), −10.76 (d, 165, 1B), −15.37 (d, 141, 1B), −19.22 (d, 153, 1B), −27.51 (d, 144, 1B), −30.94 (d, 135, 1B), −35.78 (d, 146, 1B). Anal. Calc. for $C_6H_{21}B_9S$: C, 32.38; H, 9.51; B, 43.71. Found: C, 32.12; H, 9.53; B, 43.67%.

4.4. Synthesis of 9-NMe_3-7,8-$C_2B_9H_{11}$ (**2c**)

o-Carborane (7.2 g, 0.05 mmol) was slowly added under stirring and cooling by cold water to a solution of KOH (7.5 g, 0.135 mmol) in MeOH (100–150 ml) placed in 1 L flask. The reaction mixture was stirred at room temperature until hydrogen evolution was over and was then refluxed for 4 h. The most of MeOH was removed by distillation at atmospheric pressure, water was added (50–70 ml) and the rest of the MeOH was removed in vacuum to give an aqueous alkaline solution of $K[C_2B_9H_{12}]$. Several pieces of dry ice were added to neutralize an excess of KOH. A solution of $[Me_3NH]Cl$ (9.6 g, 0.1 mmol) in H_2O (50 ml), conc. aqueous NH_3 solution (50 ml) and CH_2Cl_2 (300 ml) were added. Then, a solution of $CuSO_4 \cdot 5H_2O$ (60 g, 0.24 mmol) in H_2O (250 ml) was added dropwise under stirring within 1 h followed by addition of conc. aqueous NH_3 solution (100 ml) in one portion. The reaction mixture was stirred for 48 h. The organic layer was separated, washed with 1 M solution of HCl and dried over Na_2SO_4. The solvent was removed in vacuum to yield **2c** (8.0 g, 85%) as a white crystalline solid. The product is sufficiently pure and can be used for subsequent syntheses without purification. M.p. 258–260 °C. ^{1}H NMR ($CDCl_3$): $\delta = 3.06$ (s, 9H, NMe_3), 2.40 (br s, 1H, cage CH), 1.92 (br s, 1H, cage CH), −3.37 (v br s, 1H, μ-H). ^{11}B NMR ($CDCl_3$): $\delta = 5.36$ (s, $BNMe_3$, 1B), −5.25 (d, 140, 1B), −16.52 (d, 135, 1B), −17.23 (d, 156, 1B), −18.91 (d, 179, 1B), −24.47 (d, 151, 1B), −27.43 (d, 143, 1B), −32.25 (d, 134, 1B), −38.73 (d, 146, 1B). Anal. Calc. for $C_5H_{20}B_9N$: C, 31.36; H, 10.53; N, 7.31. Found: C, 31.92; H, 9.94; N, 7.59%. If necessary, the product can be purified by recrystallization from CH_2Cl_2/petroleum ether.

4.5. Synthesis of 9-py-7,8-$C_2B_9H_{11}$ (**2d**)

A mixture of $Cs[C_2B_9H_{12}]$ (4 g, 15 mmol), $FeCl_3 \cdot 6H_2O$ (12 g, 44.4 mmol) and pyridine (120 ml) was refluxed for 5 h. After cooling to room temperature, CH_2Cl_2 (150–200 ml) and H_2O (1 L) were added and the mixture was vigorously shaken. The organic layer was separated, washed several times with water and diluted HCl and dried with Na_2SO_4. After evaporation of the solvent, the crude product was chromatographed on silica gel column (3 × 40 cm). Elution by CH_2Cl_2 gives a slightly yellow band and subsequent elution by acetone gives a yellow-orange band. The slightly yellow band was evaporated to a small volume, heptane was added and the most of CH_2Cl_2 was removed in vacuum. White crystalline precipitate of **2d** was filtered off, washed with petroleum ether and dried in vacuum. Yield 1.93 g (61%). M.p. 160–162 °C. ^{1}H NMR (acetone-d_6): $\delta = 9.11$ (d, 5.6, 2H, py), 8.50 (t, 7.6, 1H, py), 8.02 (t, 7.2, 2H, py), 3.04 (br s, 1H, cage CH), 2.07 (br s, 1H, cage CH), −2.85 (v br s, 1H, –H). ^{11}B NMR (acetone-d_6): $\delta = 3.85$ (s, B-py, 1B), −4.62 (d, 139, 1B), −15.94 (d, 149, 2B), −18.24 (d, 164, 1B), −21.04 (d, 151, 1B), −26.18 (d, 142, 1B), −29.56 (d, 134, 1B), −36.59 (d, 144, 1B). Anal. Calc. for $C_7H_{16}B_9N$: C, 39.75; H, 7.63; N, 6.62. Found: C, 38.95; H, 7.55; N, 7.06%.

The yellow-orange band was evaporated to a small volume and petroleum ether was added to precipitate orange microcrystalline solid, which was identified as 9,11-py_2-*nido*-7,8-$C_2B_9H_9$. It decomposes in CH_2Cl_2 solution within 1 day. ^{1}H NMR (acetone-d_6): $\delta = 8.94$ (d, 5.6, 4H, py), 8.23 (t, 7.6, 2H, py), 7.82 (t, 7.2, 4H, py), 1.94 (s, 2H, cage CH). ^{11}B NMR (acetone-d_6): $\delta = -5.00$ (br, 3B, 2 + 1 coincidence), −16.85 (d, 134, 2B), −23.20 (d, 145, 2B), −26.82 (d, 154, 1B), −46.19 (d, 142, 1B).

4.6. Preparation of solutions of Na[9-L-7,8-R_2-7,8-$C_2B_9H_8$] (Na[**1a–d**]) in THF

4.6.1. Na[**1a**]

Carborane **2a** (2470 mg, 12.7 mmol) was added to a suspension of NaH (720 mg, 30 mmol) in 60 ml of THF. The reaction mixture was refluxed under stirring until hydrogen evolution was ceased (ca. 0.5 h). A colourless solution of Na[**1a**] (ca. 0.22 M) obtained in this way was stored under argon over an excess of NaH and was taken off by a syringe. In order to determine an exact concentration, an aliquot of the solution was titrated by 0.1 M H_2SO_4.

4.6.2. Na[**1b**]

A colourless solution of Na[**1b**] in THF (ca. 0.12 M) was prepared similarly to the previous procedure by refluxing a mixture of NaH (200 mg, 8.33 mmol) and **2b** (534 mg, 2.4 mmol) in 20 ml of THF for 6 h.

4.6.3. Na[**1c**]

A colourless solution of Na[**1c**] in THF (ca. 0.17 M) was prepared similarly to Na[**1a**] by refluxing a mixture of NaH (720 mg, 30 mmol) and **2c** (1910 mg, 10 mmol) in 60 ml of THF for 12 h.

4.6.4. Na[**1d**]

Carborane **2d** (507 mg, 2.4 mmol) was added to a suspension of NaH (200 mg, 8.33 mmol) in 60 ml of THF. The reaction mixture was refluxed under stirring until hydrogen evolution was ceased (ca. 1 h) to give a dark red solution of Na[**1d**] (ca. 0.04 M). The low concentration is explained by much lower solubility of Na[**1d**] compared to Na[**1a–c**].

4.7. Synthesis of Cb*Co(η-9-L-7,8-R_2-7,8-$C_2B_9H_8$) (**3a–3d**)

4.7.1. Method A (using Cb*Co$(CO)_2$I)

A solution of Na[**1a**,**c**,**d**] (0.22 mmol) in THF was added under stirring to a solution of Cb*Co$(CO)_2$I (75 mg, 0.21 mmol) in 10 ml of THF. The reaction mixture was refluxed for 12 h. The solvent was removed in vacuum and the residue was chromatographed on silica gel column using CH_2Cl_2/hexane (1:1) as an eluent. Yellow band was collected and the solvent was removed in vacuum to give a yellow-orange microcrystalline product.

4.7.2. Method B (using [Cb*Co$(MeCN)_3$]PF_6)

A solution of [Cb*Co(C_6H_6)]PF_6 (195 mg, 0.5 mmol) or [Cb*Co(C_6H_5Me)]PF_6 (202 mg, 0.5 mmol) in 10 ml of MeCN was refluxed for 12 h or irradiated (400 W mercury phosphor coated lamp, cooling by running water) for 7 h to give an orange-red solution of [Cb*Co$(MeCN)_3$]PF_6 [1]. A solution of Na[**1a–d**] (0.5 mmol) in THF was added at 0 °C and the reaction mixture was stirred overnight at room temperature. The products were isolated as described in Method A.

Complex ***3a***. L = SMe_2, R = H. Yields: 45% (Method A), 86% (Method B). ^{1}H NMR (CD_2Cl_2): $\delta = 2.80$ (br d, 1H, cage CH), 2.59 (s, 3H, SMe_2), 2.39 (s, 3H, SMe_2), 2.30 (br d, 1H, cage CH), 1.56 (s, 12H, Cb). ^{1}H NMR (acetone-d_6): $\delta = 3.04$ (br d, 1H, cage CH), 2.63 (s, 3H, SMe_2), 2.51 (s, 3H, SMe_2), 2.35 (br d, 1H, cage CH), 1.59 (s, 12H, Cb). ^{11}B NMR (CD_2Cl_2): $\delta = -6.35$ (d, 140, 1B), −9.21 (s, $BSMe_2$, 1B), −11.02 (d, 158, 1B), −13.96 (d, 144, 1B), −17.61 (d, 150, 1B), −17.61 (d, 136, 1B), −24.82 (d, 126, 1B), −26.56 (d, 128, 1B), −28.13 (d, 118, 1B). ^{11}B{^{1}H} NMR (acetone-d_6): $\delta = -4.51$ (1B), −7.69 (1B), −9.48 (1B), −12.24 (1B), −15.95 (2B), −23.33 (1B), −24.89 (1B), −26.64 (1B). Anal. Calc. for $C_{12}H_{28}B_9CoS$: C, 39.97; H, 7.83; B, 26.98; S 8.89. Found: C, 39.69; H, 7.99; B, 26.57; S, 8.50%.

Complex ***3b***. L = SMe_2, R = Me. Yield 39% (Method B). ^{1}H NMR (acetone-d_6): $\delta = 2.90$ (s, 3H, SMe_2), 2.86 (s, 3H, SMe_2), 2.68 (s, 3H, cage CMe), 2.57 (s, 3H, cage CMe), 1.47 (s, 12H, Cb). ^{11}B{^{1}H} NMR (acetone-d_6): $\delta = -3.73$ (1B), −7.03 (2B), −15.01 (2B), −16.70 (1B), −18.07 (2B), −19.73 (1B). Anal. Calc. for $C_{14}H_{32}B_9CoS$: C, 43.26; H, 8.30. Found: C, 43.41; H, 8.35%.

Complex ***3c***. L = NMe_3, R = H. Yields: 36% (Method A), 72% (Method B). ^{1}H NMR (acetone-d_6): $\delta = 3.01$ (s, 9H, NMe_3), 2.07 (br s, 1H, cage CH), 1.50 (s, 12H, Cb), 1.23 (br s, 1H, cage CH). ^{11}B{^{1}H} NMR (acetone-d_6): $\delta = 4.03$ (1B), −5.10 (1B), −10.76 (1B), −13.68 (1B), −15.77 (1B), −16.64 (1B), −24.61 (1B), −27.15 (2B). Anal. Calc. for $C_{13}H_{31}B_9CoN$: C, 43.66; H, 8.74; N, 3.92. Found: C, 44.14; H, 8.96; N 3.77%.

Complex ***3d***. L = py, R = H. Yields: 50% (Method A), 47% (Method B). ^{1}H NMR (acetone-d_6): $\delta = 8.70$ (t, 2H, py), 8.32 (t, 1H, py), 7.93 (t, 2H, py), 3.48 (br s, 1H, cage CH), 2.35 (br s, 1H, cage CH), 1.28 (s, 12H, Cb). ^{11}B{^{1}H} NMR (acetone-d_6): $\delta = -0.29$ (1B), −6.46 (1B), −11.02 (1B), −13.48 (2B), −15.90 (1B), −21.71 (1B), −26.18 (1B), −27.40 (1B). Anal. Calc. for $C_{15}H_{27}B_9CoN$: C, 47.71; H, 7.21. Found: C, 48.20; H 7.25%.

4.8. X-ray crystallography

Crystals of carborane **2d** suitable for X-ray diffraction study were grown up by slow diffusion in two-layer system, solution of complex in $CDCl_3$/petroleum ether, placed in an NMR tube. Crystals of complexes **3a** and **3d** were obtained similarly using acetone-d_6 instead of $CDCl_3$. X-ray diffraction experiments were carried out with a Bruker SMART 1000 CCD area detector, using graphite monochromated Mo Kα radiation ($l = 0.71073$ Å, ω-scans with a 0.3° step in ω and 10 s per frame exposure) at 110 K. Low temperature of the crystals was maintained with a Cryostream (Oxford Cryosystems) open-flow N_2 gas cryostat. Reflection intensities were integrated using SAINT software [23]

Table 5
Crystal data and structure refinement parameters for **2d**, **3a** and **3d**

Compound	**2d**	**3a**	**3d**
Empirical formula	$C_7H_{16}B_9N$	$C_{12}H_{28}B_9CoS$	$C_{15}H_{27}B_9CoN$
Formula weight	211.50	360.64	377.61
Crystal colour, habit	Pale yellow prism	Red prism	Red prism
Crystal size (mm)	$0.41 \times 0.31 \times 0.15$	$0.43 \times 0.32 \times 0.30$	$0.38 \times 0.35 \times 0.29$
Temperature (K)	120(2)	100(2)	120(2)
Crystal system	Monoclinic	Monoclinic	Monoclinic
Space group	$P2_1/n$	$P2_1/n$	$P2_1/n$
a (Å)	10.200(2)	11.619(1)	16.215(5)
b (Å)	8.5432(17)	13.622(1)	12.370(3)
c (Å)	14.605(3)	11.799(1)	9.528(3)
β (°)	104.90(3)	103.017(2)	91.678(6)
V (Å^3)	1229.9(4)	1819.5(3)	1910.4(9)
Z (Z')	4(1)	2(1)	4(1)
$F(000)$	440	752	784
D_{calc} (g cm^{-3})	1.142	1.046	1.313
μ (cm^{-1})	0.55	10.46	8.96
T_{min}/T_{max}	0.9648/0.9079	0.9252/0.8503	0.847/0.721
Scan type	ω	ω	ω
θ Range (°)	3.57–29.00	2.22–30.00	1.29–30.00
Completeness of dataset (%)	99.0	99.0	99.2
Reflections measured	8989	46818	22257
Independent reflections	3224 [$R_{int} = 0.0559$]	5263 [0.0229]	5528 [0.0397]
Observed reflections [$I > 2\sigma$ (I)]	2254	5091	3967
Parameters	218	320	343
R_1 (on F for obs. refls)	0.0634	0.0201	0.0457
wR_2 (on F^2 for all refls)	0.1509	0.0546	0.1097
GOF	0.999	1.060	1.089
$\Delta\rho_{max}$ $\Delta\rho_{min}$ (e Å^{-3})	0.354, −0.262	0.441, −0.181	0.691, −0.384

and absorption correction was applied semi-empirically using SADABS program [24]. The structures were solved by direct method and refined by the full-matrix least-squares against F^2 in anisotropic approximation for non-hydrogen atoms. All polyhedron hydrogen atoms were located from the Fourier density synthesis and refined in isotropic approximation. Crystal data and structure refinement parameters for **2d**, **3a** and **3d** are given in Table 5. All calculations were performed using the SHELXTL software [25].

5. Supplementary material

The crystallographic data have been deposited with the Cambridge Crystallographic Data Center, CCDC 255386 for **2d**, CCDC 255387 for **3a** and CCDC 255388 for **3d**. Copies of this information may be obtained free of charge from: The Director, CCDC, 12 Union Road, Cambridge, CB2 1EZ, UK (Fax: +44 1223 336033; e-mail: deposit@ccdc.cam.ac.uk or http://www.ccdc.cam.ac.uk).

Acknowledgements

A.R.K. is grateful to General Chemistry and Material Science Division of Russian Academy of Sciences for financial support (Grant No. 05-07). P.Z. gratefully acknowledges the financial support from Università di Siena (PAR 2003). Z.J. thanks Ministry of Education of the Czech Republic (Grant No. LN00A0280).

References

[1] E.V. Mutseneck, D.A. Loginov, D.S. Perekalin, Z.A. Starikova, D.G. Golovanov, P.V. Petrovskii, P. Zanello, M. Corsini, F. Laschi, A.R. Kudinov, Organometallics 23 (2004) 5944.
[2] (a) For recent reviews, see R.N. Grimes, in: G. Wilkinson, F.A.G. Stone, E.W. Abel (Eds.), Comprehensive Organometallic Chemistry, vol. 1, Pergamon Press, Oxford, 1982, p. 459;
(b) R.N. Grimes, in: E.W. Abel, F.A.G. Stone, G. Wilkinson (Eds.), Comprehensive Organometallic Chemistry II, vol. 1, Pergamon Press, Oxford, 1995, p. 373;
(c) A.K. Saxena, N.S. Hosmane, Chem. Rev. 93 (1993) 1081;
(d) A.K. Saxena, J.A. Maguire, N.S. Hosmane, Chem. Rev. 97 (1997) 2421.
[3] I.B. Sivaev, V.I. Bregadze, Collect. Czech. Chem. Commun. 64 (1999) 783.
[4] R. Hoffmann, Angew. Chem., Int. Ed. Engl. 21 (1982) 711.
[5] (a) J. Plešek, Z. Janoušek, S. Heřmanék, Coll. Czech. Chem. Commun. 43 (1978) 2862;
(b) Y.-K. Yan, D.M.P. Mingos, T.E. Müller, D.J. Williams, M. Kurmoo, J. Chem. Soc., Dalton Trans. (1994) 1735.
[6] D.C. Young, D.V. Howe, M.F. Hawthorne, J. Am. Chem. Soc. 91 (1969) 859.
[7] A.R. Kudinov, D.S. Perekalin, P.V. Petrovskii, K.A. Lyssenko, G.V. Grintselev-Knyazev, Z.A. Starikova, J. Organomet. Chem. 657 (2002) 115 (and references therein).

[8] H.C. Kang, S.S. Lee, C.B. Knobler, M.F. Hawthorne, Inorg. Chem. 30 (1991) 2024.
[9] Z. Janoušek, J. Plešek, S. Heřmánek, B. Štíbr, Coll. Czech. Chem. Commun. 39 (1974) 2363.
[10] V.I. Meshcheryakov, K.A. Lyssenko, G.V. Grintselev-Knyazev, P.V. Petrovskii, A.R. Kudinov, in: Yu.N. Bubnov (Ed.), Boron Chemistry at the Beginning of the 21st Century, URSS, Moscow, 2003, p. 255.
[11] Synthesis of **3a** was described in a short communication A.R. Kudinov, V.I. Meshcheryakov, P.V. Petrovskii, M.I. Rybinskaya, Izv. Akad. Nauk Ser. Khim. (1999) 177;
A.R. Kudinov, V.I. Meshcheryakov, P.V. Petrovskii, M.I. Rybinskaya, Russ. Chem. Bull. 48 (1999) 176 (Engl. Transl.).
[12] The thallium derivative Tl[**1d**] was prepared by reaction of carborane **2d** with TlOAc/KOH in DMSO/H_2O, similar to the preparation of Tl[**1a**] E.J.M. Hamilton, A.J. Welch, Polyhedron 10 (1991) 471.
[13] M.V. Butovskii, U. Englert, A.A. Fil'chikov, G.E. Herberich, U. Koelle, A.R. Kudinov, Eur. J. Inorg. Chem. (2002) 2656.
[14] A.R. Kudinov, E.V. Mutseneck, D.A. Loginov, Coord. Chem. Rev. 248 (2004) 571 (and references therein).
[15] J. Cowie, E.J.M. Hamilton, J.C.V. Laurie, A.J. Welch, Acta Crystallogr., Sect. C 48 (1988) 1648.
[16] P.A. Jelliss, F.G.A. Stone, J. Organomet. Chem. 500 (1995) 307.
[17] M. Corsini, P. Zanello, A.R. Kudinov, V.I. Meshcheryakov, D.S. Perekalin, K.A. Lyssenko, J. Solid State Electrochem. (Available online July 12, 2005).
[18] P. Zanello, Inorganic Electrochemistry. Theory, Practice and Application, RSC, Cambridge, 2003.
[19] (a) F.E. Mabbs, D. Collison, Electron Paramagnetic Resonance of d Transition Metal Compounds, Studies in Inorganic Chemistry, vol. 16, Elsevier, New York, 1992;
(b) R.S. Drago, Physical Methods for Chemists, Saunders College Publishing, New York, 1992.
[20] A. Bencini, D. Gatteschi, ESR Spectra of Metal Complexes of the First Transition Series in Low-Symmetry Environments, Transition Metal Chemistry. A Series of Advances, vol. 8, Marcel Dekker Inc, New York, 1982.
[21] P. Zanello, F. Laschi, M. Fontani, C. Mealli, A. Ienco, K. Tang, X. Jin, L. Li, J. Chem. Soc., Dalton Trans. (1999) 965.
[22] M. Krejèik, M.F. Danek, F. Hartl, J. Electroanal. Chem. 317 (1991) 179.
[23] SMART V5.051 and SAINT V5.00, Area Detector Control and Integration Software, Bruker AXS Inc., Madison, WI, USA, 1998.
[24] G.M. Sheldrick, SADABS, Bruker AXS Inc., Madison, WI, USA, 1997.
[25] G.M. Sheldrick, SHELXTL-97, Version 5.10, Bruker AXS Inc., Madison, WI, USA, 1997.